JMEPEG (2012) 21:671–677
DOI: 10.1007/s11665-012-0122-6

1059-9495/$19.00

Active Metal Brazing of Machinable Aluminum Nitride-Based Ceramic to Stainless Steel

Aníbal Guedes and Ana Maria Pires Pinto

(Submitted September 29, 2011; in revised form December 14, 2011)

Shapal™-M machinable AlN-based ceramic and AISI 304 stainless steel were joined by active metal brazing, at 750, 800, and 850 °C, with a dwell stage of 10 min at the processing temperature, using a 59Ag-27.25Cu-12.5In-1.25Ti (wt.%) filler foil. The influences of temperature on the microstructural features of brazed interfaces and on the shear strength of joints were assessed. The interfacial microstructures were analyzed by scanning electron microscopy (SEM), and the composition of the phases detected at the interfaces was evaluated by energy dispersive X-ray spectroscopy (EDS). The fracture surfaces of joints were analyzed by SEM, EDS, and GIXRD (Grazing Incidence X-Ray Diffraction). Reaction between the liquid braze and both base materials led to the formation of a Ti-rich layer, adjacent to each base material. Between the Ti-rich layers, the interfaces consist of a (Ag) solid-solution matrix, where coarse (Cu) particles and either Cu-In or Cu-In-Ti and Cu-Ti intermetallics phases are dispersed. The stronger joints, with shear strength of 220 ± 32 MPa, were produced after brazing at 800 °C. Fracture of joints occurred preferentially not only through the ceramic sample but also across the adjoining TiN layer, independent of the brazing temperature.

Keywords brazing, mechanical testing, stainless steels, structural ceramics

1. Introduction

Aluminum nitride (AlN) exhibits, among ceramics, a unique combination of properties such as high thermal conductivity, high electrical resistivity, low coefficient of thermal expansion, low dielectric constant (Ref 1), large band gap, good thermal shock resistance, and excellent corrosion resistance to plasma and halogen gases (Ref 1, 2). Applications of AlN include electronic substrates and packaging, high-frequency acoustic wave devices, light-emitting diodes, and wide band gap semiconductors (Ref 1). A new promising application of AlN is as a biosensing film for use in wireless technology for monitoring cell, since it performs effectively in biosensing and biophysical detection (Ref 3). AlN is also reported to be an efficient material for nuclear applications (Ref 4, 5). However, like other ceramics, AlN is intrinsically brittle and thus, production of AlN components with intricate shape is problematic. In addition, the low bending strength of AlN hinders its application as a structural material. Shapal™-M (Goodfellow, United Kingdom) is a machinable AlN-based ceramic with a bending strength of almost 300 MPa, which is comparable to that of alumina, with the advantage of possessing a five-time higher thermal conductivity. The machinability and strength of Shapal™-M enable its prospective use in structural applications; this will inevitably require the processing of joints between Shapal™-M and other materials. For instance, as AlN (Ref 6), the joining of Shapal™-M to stainless steels may be required for thermomechanical applications. Therefore, it is most important to assess the possibility of producing sound Shapal™-M joints that present adequate mechanical properties. Brazing (Ref 6-8), active metal brazing (Ref 6, 9-11), copper direct bonding (Ref 6, 12-14), transient liquid phase bonding (Ref 15), and diffusion bonding (Ref 7, 16, 17), have been reported to be adequate techniques to join AlN. These joining routes may be suitable to produce Shapal™-M joints but, to our best knowledge, there are no reports that ascertain this hypothesis.

The main aims of the study reported in this article are to assess the suitability of using Incusil-ABA (MTC Wesgo Metals, United States), which is an active brazing alloy based on Ag-Cu eutectic alloyed with In and Ti, as filler for joining Shapal™-M to AISI 304 stainless steel (Goodfellow, United Kingdom) and to determine the influence of the processing temperature upon the microstructural features of the interfaces and on the mechanical strength of joints.

2. Materials and Experimental Procedures

Samples of Shapal™-M (70AlN-30BN, wt.%) and of AISI 304 stainless steel (Fe-18Cr-10Ni-0.04C, wt.%), with 10 and 12.7 mm in diameter, respectively, were cut with a low-speed diamond saw to a thickness of 5 mm and then ground with SiC emery paper down to 4000 grade. A 100-μm-thick foil of Incusil-ABA (59Ag-27.25Cu-12.5In-1.25Ti, wt.%) was used as

This article is an invited submission to JMEP selected from presentations at the Symposia "Wetting, soldering and brazing" and "Diffusion bonding and characterization" belonging to the Topic "Joining" at the European Congress and Exhibition on Advanced Materials and Processes (EUROMAT 2011), held September 12-15, 2011, in Montpellier, France, and has been expanded from the original presentation.

Aníbal Guedes and **Ana Maria Pires Pinto**, Department of Mechanical Engineering, University of Minho, CT2M, Campus de Azurém, Guimarães 4800-058, Portugal. Contact e-mails: aguedes@dem.uminho.pt and anapinto@dem.uminho.pt.

filler. The foil was cut into disks with the same diameter as that of Shapal™-M samples. Before brazing, all materials were cleaned in acetone with ultrasonic agitation and dried in air. A contact pressure of 2.9 x 10^4 Pa was applied, by means of a stainless steel mass, to the brazing assemblage that consisted of a Shapal™-M/Incusil-ABA/AISI 304 stainless steel sandwich. The assemblage was inserted into the chamber of an electrical furnace that was evacuated to a vacuum level that remained greater than 10^{-2} Pa during the entire brazing thermal cycle. Brazing was performed at 750, 800, and 850 °C with a 10-min dwelling stage; the heating and cooling rates were set to 3 °C min^{-1} by a temperature controller.

Joints for microstructural and chemical characterization were cross-sectioned perpendicularly to the interface, cold mounted in epoxy resin, and then prepared according to standard metallographic techniques. The microstructure and the chemical composition of the interfaces were analyzed on a FEI Nova 200 scanning electron microscope, equipped with an EDAX-Pegasus energy dispersive spectrometer. EDS analysis were performed at an accelerating voltage of 15 keV, using conventional ZAF correction procedure included in the EDAX-Pegasus software.

Samples of Shapal™-M and of AISI 304 stainless steel with 12-mm length were brazed for shear testing. Shear testing was conducted at room temperature with a crosshead speed of 5 mm min^{-1}. At least, five samples were tested for each brazing temperature. Additional details on the shear test apparatus are given elsewhere (Ref 18). The fracture surfaces were examined by SEM, EDS, and GIXRD (Grazing Incidence X-Ray Diffraction) performed at 40 kV and 40 mA, using Cu Kα radiation.

For the sake of convenience, Shapal™-M and AISI 304 stainless steel will be referred hereafter as SM and SS, respectively.

3. Results and Discussion

Typical microstructures of the interfaces obtained after joining at the different processing temperatures tested in this investigation are shown in Fig. 1. All brazing temperatures induced the formation of interfaces with no apparent porosity and free of cracks. The interfaces could be divided into three different zones: the central zone, and the thin reaction layers formed near the base materials—one adjacently to SM and the other contiguously to the SS sample. The reaction layers are barely detectable after brazing at 750 °C, since they are extremely thin and not continuous. Near SM, the extension of reaction layer, which is at the most 4 μm thick, slightly increases with the increment in brazing temperature. However, the thickness of reaction layer formed contiguously to SS remained less than 1 μm for all brazing temperatures. The extension of the interface decreases as the brazing temperature is incremented. The interfaces are about 85, 55, and 25 μm thick, for brazing at 750, 800, and 850 °C, respectively, as observed in Fig. 1. It should be noted that due to the open end configuration of joints, the liquid filler is free to flow out of the joint gap. In addition to that, the contact pressure applied to the joining assemblage may also enhance overflowing. Since the fluidity of molten filler increases as the brazing temperature is incremented, a higher volume fraction of molten braze will be lost causing the overall extension of the interface to decrease. A similar evolution of the width of the interface was reported when Incusil-ABA was used to produce titanium/steel

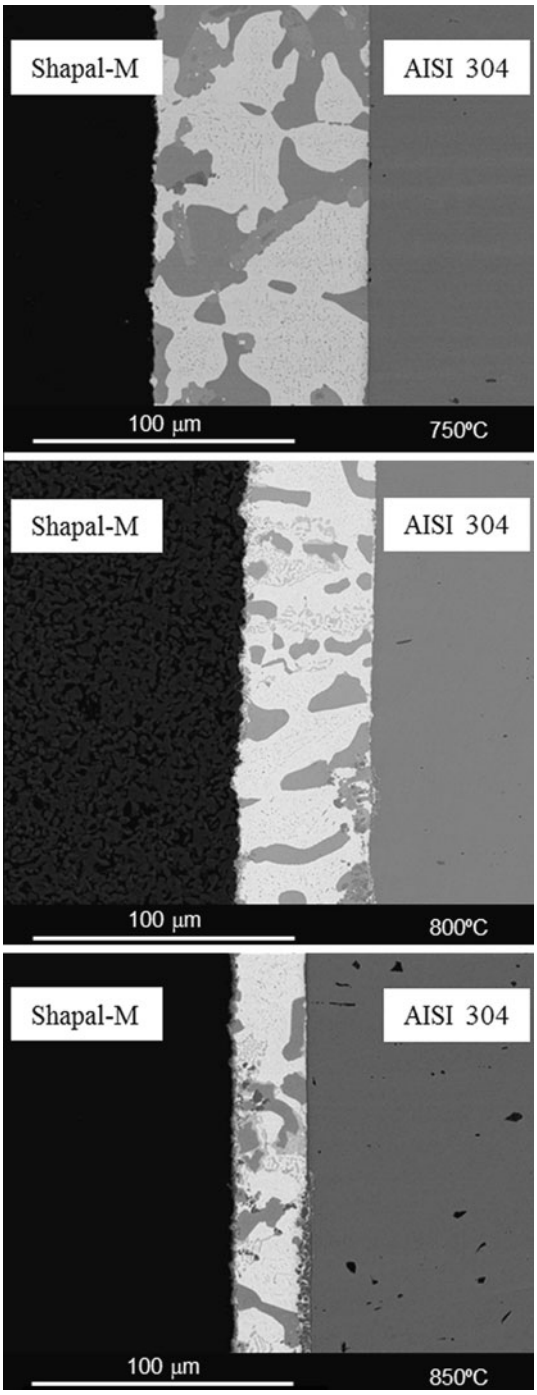

Fig. 1 Backscattered electron images (BEIs) of the interfaces after joining at different temperatures

joints (Ref 19); the configuration of joints and the brazing temperatures were the same as those used in the present study.

By the analysis of Fig. 2 and 3, where the elemental distributions across the interface are presented for the two limiting temperatures tested, it can be concluded that there was little interdiffusion between the base materials and the braze alloy. In addition, it can be observed that Ti atoms tend to migrate toward the vicinity of both base materials. The diffusivity of Ti increases with temperature increment, and thus, the central zone of the interface becomes progressively depleted in Ti as the brazing temperature is raised. Figure 3 is

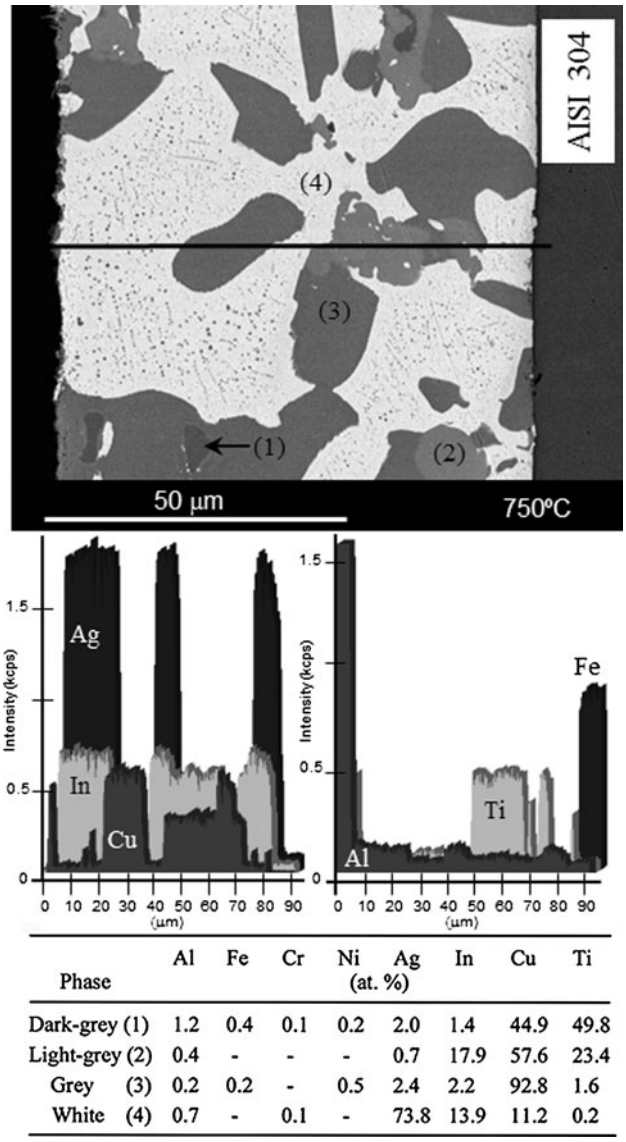

Phase	Al	Fe	Cr	Ni	Ag	In	Cu	Ti
	(at. %)							
Dark-grey (1)	1.2	0.4	0.1	0.2	2.0	1.4	44.9	49.8
Light-grey (2)	0.4	-	-	-	0.7	17.9	57.6	23.4
Grey (3)	0.2	0.2	-	0.5	2.4	2.2	92.8	1.6
White (4)	0.7	-	0.1	-	73.8	13.9	11.2	0.2

Fig. 2 X-ray elemental line scan profiles across the interface and chemical compositions of phases detected after brazing at 750 °C

particularly elucidative regarding the segregation of Ti and the formation of Ti-rich reaction layers adjacently to both SM and SS samples.

Semi-quantitative SEM/EDS analysis was used in conjunction with ternary phase diagrams to evaluate the nature of the phases detected at the central zone of the interfaces. Results of EDS analysis performed on several phases detected after brazing at 750 °C are presented in Fig. 2. As observed in the figure, the central zone of the interface is composed of a mixture consisting of a white phase and several gray phases. The white phase is rich in Ag and In and should consist of (Ag) solid solution, since its composition lies on the (Ag) single-phase field of the Ag-Cu-In isothermal section presented in Fig. 4. The gray phase is (Cu) solid solution and the dark-gray phase, which is indicated by an arrow in Fig. 2, should consist of CuTi intermetallic compound. The light-gray phase is predominantly composed of Cu, Ti, and In. The Cu-In-Ti phase diagram is still to be established, and the only known compound belonging to this system is Cu_2InTi (Ref 20). The

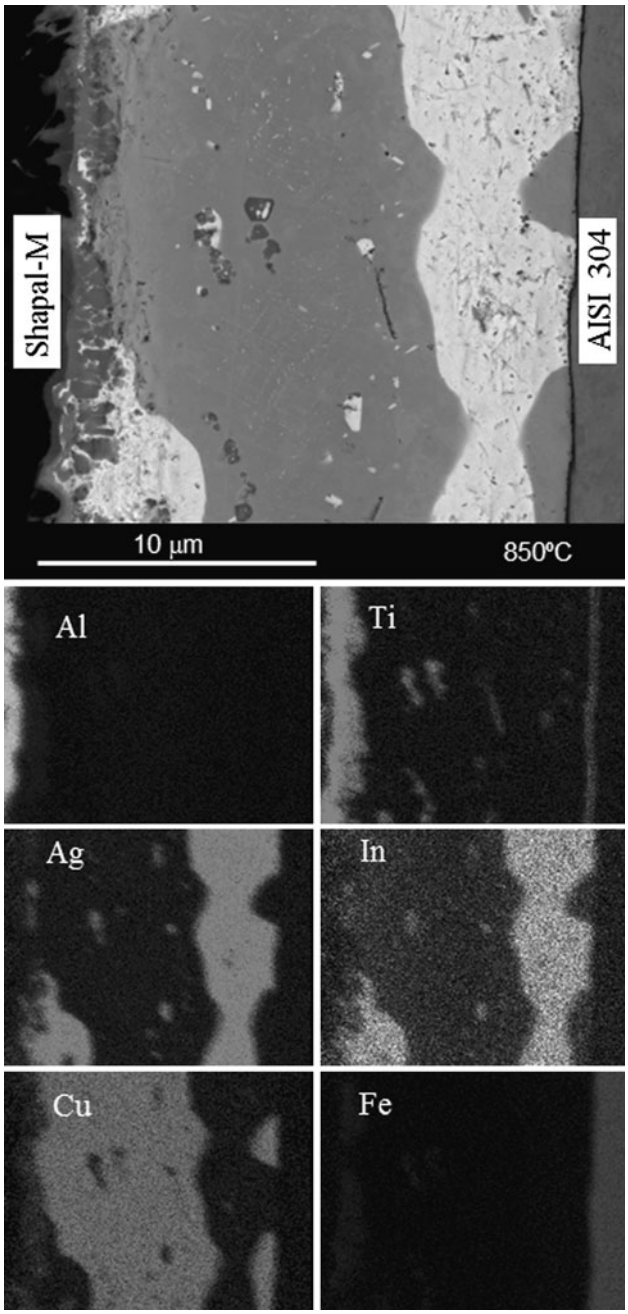

Fig. 3 X-ray diffraction elemental maps of the interface after brazing at 850 °C

phase detected in the present investigation is richer in Cu, and poorer in In than Cu_2InTi, since its stoichiometry is, approximately, $Cu_{2.5}In_{0.8}Ti$. However, the interactions of Cu-rich zones located below and around the light-gray phase may induce slightly misleading EDS results. Thus, the light-gray phase may be less rich in Cu than is indicated by EDS analysis, and therefore, its composition may be in fact closer to that of Cu_2InTi.

For joining either at 800 and 850 °C, the central zone of the interface consists mainly of a mixture of (Ag) and (Cu) solid solutions and Cu-In-rich phase; no Cu-In-Ti phase was detected. The composition of the Cu-In-rich phase (7.4Ag-64.2Cu-26.9In, at.%) lies near the Cu_7In_3 single-phase field on the Ag-Cu-In isothermal section presented in Fig. 4, where it is

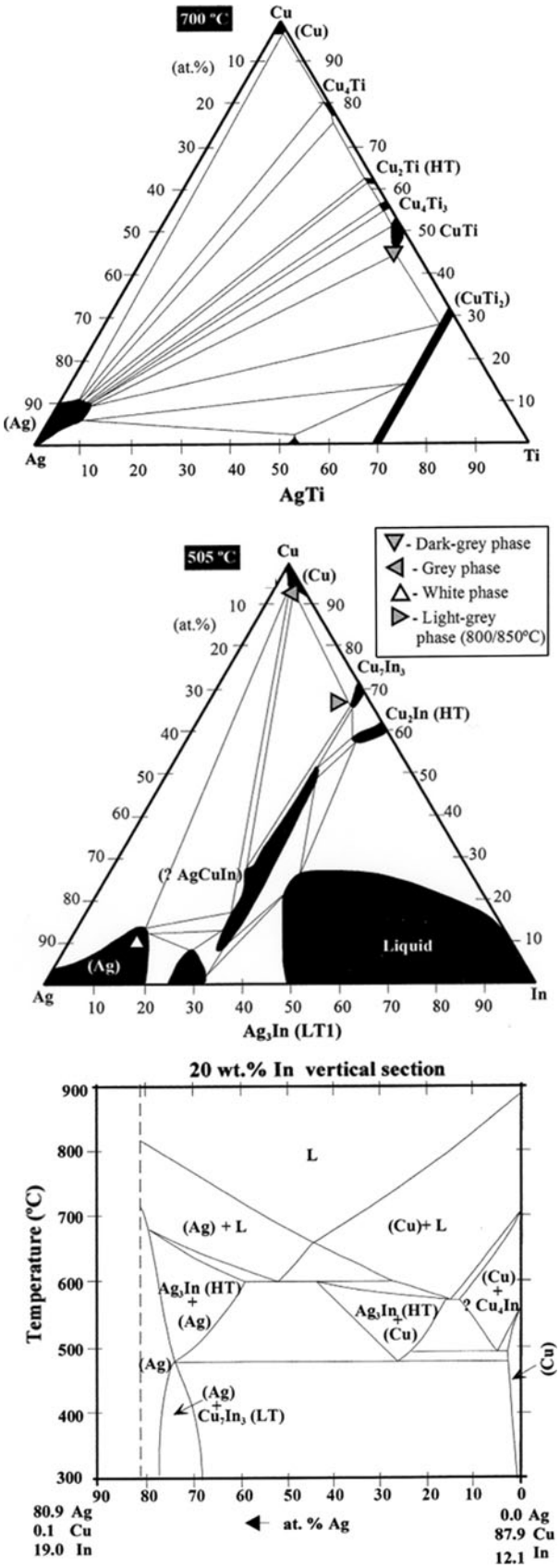

Fig. 4 Isothermal sections of the Ag-Cu-Ti and Ag-Cu-In diagrams, where the compositional plots of some of the reaction products are marked, and 20 wt.% In vertical section of the Ag-Cu-In diagram. Adapted from Ref 20

referred as the light-gray phase. The detection of (Ag), (Cu), and Cu_7In_3 phases at the center of the interface is in agreement with the Ag-Cu-In vertical section shown in Fig. 4, which indicates that these phases may coexist in equilibrium.

The bridging between the central zone of the interface and either SM or SS sample is promoted by the formation of a thin Ti-rich layer. The formation of a thin Ti-rich layer adjacently to aluminum nitride after joining either by active metal brazing (Ref 6, 7, 9, 10) or by transient liquid phase bonding (Ref 15), using Ti-activated brazing alloys, is reported in several studies. TiN was found to be the main phase of the reaction layer detected near aluminum nitride, and it would result from the following reaction:

$$\mathrm{AlN} + \mathrm{Ti} \Leftrightarrow \mathrm{Al} + \mathrm{TiN} (\Delta G_{\mathrm{T}}^{0} = -9835 - 23.4T,\ \mathrm{J\,mol^{-1}})$$

Data collected from (Ref 21) were used to calculate the standard Gibbs free energy variation ($\Delta G_{\mathrm{T}}^{0}$) of the reaction. For all brazing temperatures tested in this investigation, the reaction is, for standard conditions, thermodynamically favorable: −33.8, −35.0, and −36.2 kJ mol^{-1} at 750, 800, and 850 °C, respectively; these values are in good agreement with those reported by Dezellus et al. (Ref 15). Thus, the reaction of AlN from SM with Ti atoms that are dissolved into the melt may induce the formation of a TiN layer, and the dissolution of Al atoms into the remaining liquid filler. It should be noted that Ti-rich layer is often reported to be composed of two sublayers: a layer of TiN (Ref 22) or $TiN_{0.67}$ (Ref 15) formed contiguously to the ceramic, and another layer mainly consisting of a quaternary phase $(Ti, Cu, Al)_6N$ (Ref 15, 22) adjacent to it. In the present investigation, when brazing is carried out at 850 °C, Ti-rich layer occasionally seems to present a layered morphology (see Fig. 3). However, it was impossible to assess the composition of each sublayer, since they were less than 1 μm thick wherever this apparent morphology was observed at the interface.

SM is composed of AlN (70%, wt.%) and of BN (30%, wt.%). Therefore, interfacial reaction products may also result from the reaction of the liquid braze with BN. Ding et al. (Ref 23) studied the joining of cubic BN by active metal brazing, using a Ti-activated filler at temperatures ranging between 880 and 920 °C. Those authors reported that the reaction between the liquid braze and cubic BN induced the formation of TiN and TiB_2 at the reaction layer detected near the ceramic. Further, according to the same authors (Ref 24), the formation TiN and TiB_2 may result from following reaction:

$$\mathrm{BN} + \frac{3}{2}\mathrm{Ti} \Leftrightarrow \mathrm{TiN} + \frac{1}{2}\mathrm{TiB_2}$$

This reaction is thermodynamically viable at 600, 800, and 950 °C, since the corresponding ΔG_T^0 values are −235.34, −241.19, and −230.73 kJ mol^{-1} (Ref 24).

The results of Ding et al. (Ref 23, 24) suggest that in the present investigation, BN may have reacted with Ti from the liquid braze, promoting the formation of reaction products near SM sample, since the brazing temperatures tested were in the range of 600-950 °C. Considering these studies (Ref 15, 22-24), TiN phase would result from the reaction between Ti and either AlN or BN crystals, while TiB_2 would only result from the reaction between Ti and BN. As will be discussed latter, contrarily to TiB_2, the formation of TiN at the interface was confirmed by GIXRD analysis performed on the fracture surfaces of the joints. Therefore, Ti-rich layer should be mainly

composed of TiN and may essentially result from the reaction with AlN, since Al was detected at the interface, while TiB_2 was not identified.

Regarding the nature of Ti-rich layer located near SS, Fe35Cr13Ni3Ti7 and FeTi phases were detected by Kar et al. (Ref 25) after joining AISI 304 to Al_2O_3 by active metal brazing. Joining was performed at higher temperatures (900 and 1000 °C) than those tested in the present investigation, and the active brazing alloy used was richer in Ti (4%, wt.%). Consequently, higher reaction rate between the liquid braze and AISI 304 was achieved, and the formation of thicker (12 μm) Ti-rich layer near the stainless steel sample was observed. In the present investigation, Ti-rich layer near SS is less than 1 μm thick; the formation of Fe35Cr13Ni3Ti7 and/or FeTi intermetallic was impossible to confirm, but it could not be discarded.

It is well established that the strengths of metal/ceramic joints tend to increase as the reactions products formed near the base materials (essentially those formed near the ceramic) grow and integrate into one of more reaction layers (Ref 26). However, these reaction layers are usually composed of extremely hard and brittle phases, and their excessive thickening will cause degradation of the mechanical properties of the joints. This is primarily because these phases have little or no capacity of accommodating the residual stresses that derive predominantly from mismatches between the coefficients of thermal expansion (CTE) of the ceramic and metal samples. Thus, after reaching the maximum strength, the joints weaken because the interface becomes gradually more brittle as the volume fraction of hard reaction products increases.

The strength of joints obtained in the present investigation follows a similar trend. When joints are processed at 750 °C, the shear strength is only 148 ± 40 MPa, probably because the layer composed mainly of TiN formed contiguously to SM is still too thin and discontinuous to maximize the bonding strength. The maximum shear strength (220 ± 32 MPa) is obtained after brazing at 800 °C. At this processing temperature, TiN layer near SM is thick and continuous enough to promote the formation of stronger joints. In addition, the center of the interface still preserves a high capacity of buffering CTE mismatches (according to the Goodfellow's catalogue, CTE of SM and SS at 20 °C are, 5.2×10^{-6} and 18×10^{-6} K^{-1}, respectively). After brazing at 850 °C, the flowing of the liquid braze out of the joint gap induces a substantial decrease of the volume fraction of soft and ductile phases, like (Ag) solid solution, which is mainly detected at the center of the interface, in comparison to the interfaces produced at lower temperatures, as can be inferred by the analysis of Fig. 1. Consequently, the interface becomes more brittle and loses part of its capacity in accommodating CTE mismatches. Thus, after joining at 850 °C, the shear strength of joints (168 ± 47 MPa) decreases, in comparison to those processed at 800 °C.

In spite of the differences between the strength of joints produced under different brazing temperatures, the fracture mode remained the same. The joints fractured partially across the interface and partially throughout the SM sample, which broke into several pieces. The fracture surface of SM samples was partially covered with a thin black layer of reaction products, while the SS side of the fracture surface was covered by a thicker layer with small fragments of SM still joined to it. Figure 5 shows a fractograph of the SM side of the joints; the bulk of SM is observed in zone marked as Z1, whereas zone marked as Z2 is partially covered by reaction products. Thus,

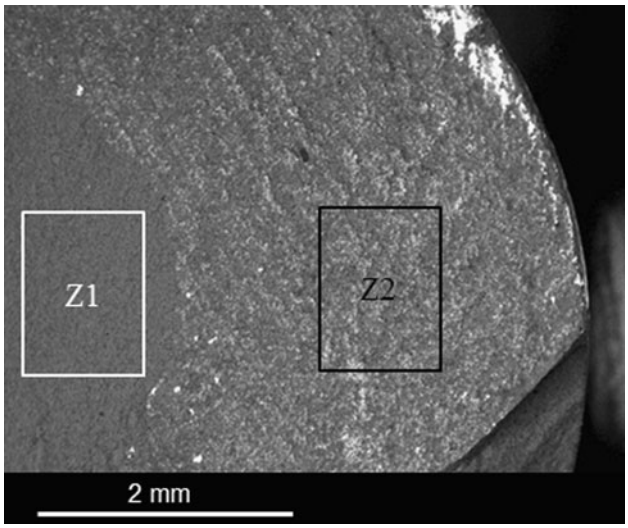

Fig. 5 BEI of the fracture surface on the AlN side of the joints after brazing at 800 °C

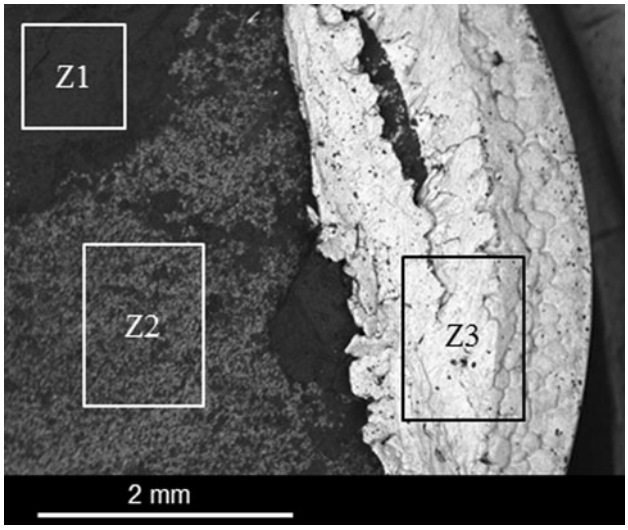

Fig. 6 BEI of the fracture surface on the SS side of the joints after brazing at 800 °C

part of the interface is included on the ceramic side of the fracture surface. The fractograph of the SS side of the joints is presented in Fig. 6. As observed in the figure, there are fragments of SM (Z1) attached to the SS sample, which is partially covered by reaction products (Z2). In addition, part of braze alloy (Z3) that has spread out of the joint gap is also observed at the periphery of the fracture surface. These observations show that fracture occurred partially across the interface and partially throughout the SM sample. GIXRD spectra of the fracture surfaces presented in Fig. 7 confirm the presence of AlN on the SM side and of AlN and TiN phases on the SS side. It should be noted that AlN and TiN present 2θ peaks very close to each other around 59°, and so it is very difficult to differentiate them. On the fracture surface of SM, this diffraction peak was assumed to result only from AlN-

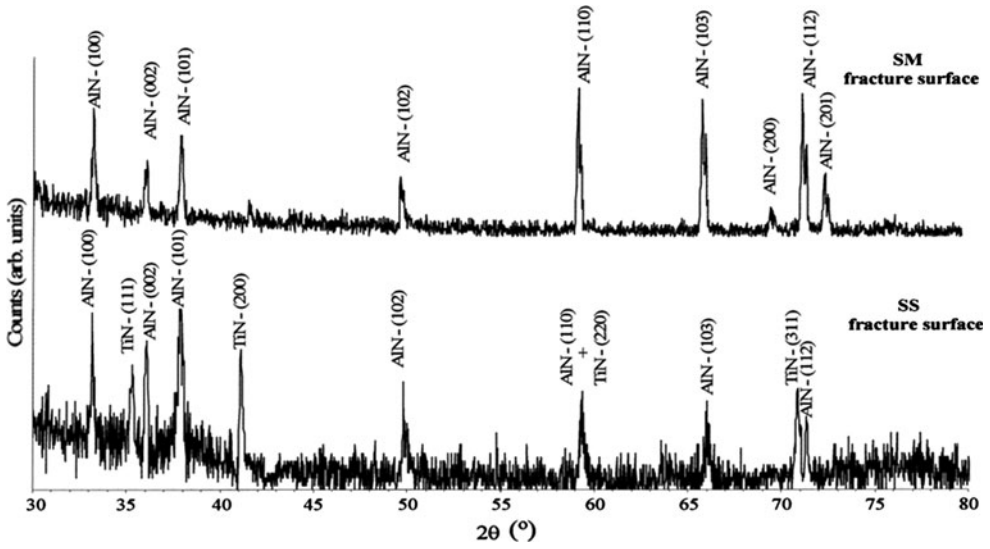

Fig. 7 GIXRD spectra (Cu Kα) of the fracture surfaces on the SM and SS sides of joints brazed at 800 °C

(110) diffraction plane, since no other TiN peak was detected, while on the SS side, it was considered to result also form TiN-(220) diffraction plane. TiN was not detected on the SM side, probably because the amount of reaction products on the thin layer that covers the SM fracture surface is not enough to produce identifiable diffraction peaks. The detection of AlN and TiN on the SS side of the fracture surface indicates that fracture of joints occurred partially throughout the SM sample, and partially across the TiN layer. Therefore, these are the critical parts of the joining: at the interface, crack nucleation and propagation should be eased at brittle TiN layer; cracks that eventually penetrate into the adjoining SM sample will cause disastrous failure of the joints.

4. Conclusions

(1) Joining Shapal™-M to AISI 304 stainless steel by active metal brazing, using 59Ag-27.25Cu-12.5In-1.25Ti (wt.%) as brazing filler, at 700, 800, and 850 C, with a dwelling stage of 10 min at the processing temperature, produces interfaces apparently free of pores and cracks.

(2) Bonding to Shapal™ is promoted by the formation of a layer with less than 4 lm thick that should be mainly composed of TiN.

(3) Bonding to AISI 304 stainless steel is promoted by the formation of a Ti-rich layer with less than 1 μm thick. (4) The central zone of the interface is mainly composed of (Ag), (Cu), and Cu_2InTi for brazing at 750 °C and of (Ag), (Cu), and Cu_7In_3 for joining at 800 and 850 °C.

(4) Fracture of joints always occurs partially across the Shapal™-M sample and partially across the adjoining TiN layer; these are the critical parts of the joints.

(5) The average shear strength of joints at room temperature is at least 148 ± 40 MPa and is maximized after brazing at 800 °C (220 ± 32 MPa).

References

1. C.-Y. Hsieh, C.-N. Lin, S.-L. Chung, J. Cheng, and D. Agrawal, Microwave Sintering of AlN Powder Synthesized by a SHS Method, *J. Eur. Ceram. Soc.*, 2007, **27**, p 343–350
2. M. Kida, M. Bahraini, J.M. Molina, L. Weber, and A. Mortensen, High-Temperature Wettability of Aluminum Nitride During Liquid Metal Infiltration, *Mater. Sci. Eng. A*, 2008, **495**, p 197–202
3. C.-C. Chen, C.-T. Lin, S.-Y. Lee, L.-H. Lin, C.-F. Huang, and K.-L. Ou, Biosensing of Biophysical Characterization by Metal-Aluminum Nitride-Metal Capacitor, *Appl. Surf. Sci.*, 2007, **253**, p 5173–5178
4. A. Gusarov, S. Huysmans, L. Vermeeren, E.R. Hodgson, and M. Decréton, In situ In-Reactor Testing of Potential Bolometer Materials for ITER Plasma Diagnostics, *Fus. Eng. Des.*, 2007, **82**, p 1179–1184
5. G. Stancari, S. Veronesi, L. Corradi, S.N. Atutov, R. Calabrese, A. Dainelli, E. Mariotti, L. Moi, S. Sanguinetti, and L. Tomassetti, Production of Radioactive Beams of Francium, *Nucl. Instrum. Methods Phys. Res. A*, 2006, **557**, p 390–396
6. A. Kara-Slimane, D. Juve, E. Leblond, and D. Treheux, Joining of AlN with Metals and Alloys, *J. Eur. Ceram. Soc.*, 2000, **20**, p 1829–1936
7. S. Zhu and W. Wlosinski, Joining of AlN Ceramic to Metals Using Sputtered Al or Ti Film, *J. Mater. Process. Technol.*, 2001, **109**, p 277–282
8. A. Koltsov, F. Hodaj, and N. Eustathopoulos, Brazing of AlN to SiC by a Pr Silicide: Physicochemical Aspects, *Mater. Sci. Eng. A*, 2008, **495**, p 259–264
9. A. Palit and M. Meier, Reaction Kinetics and Mechanical Properties in the Reactive Brazing of Copper to Aluminum Nitride, *J. Mater. Sci.*, 2006, **41**, p 7197–7209
10. N. Taranets and H. Jones, Wettability of Aluminium Nitride Based Ceramics of Different Porosity by Two Active Silver Based Brazing Alloys, *Mater. Sci. Eng. A*, 2004, **379**, p 251–257
11. M. Nicholas, D. Mortimer, L. Jones, and R. Crispin, Some Observations on the Wetting and Bonding of Nitride Ceramics, *J. Mater. Sci.*, 1990, **25**, p 2679–2689
12. W. Olesinska, D. Kalinski, M. Chmielewski, R. Diduszko, and W. Włosinski, Influence of Titanium on the Formation of a "Barrier" Layer During Joining an A1N Ceramic with Copper by the CDB Technique, *J. Mater. Sci.: Mater. Electron.*, 2006, **17**, p 781–788
13. J. Jarrige, T. Joyeux, J.P. Lecompte, and J.C. Labbe, Comparison Between Two Processes Using Oxygen in the Cu/AlN Bonding, *J. Eur. Ceram. Soc.*, 2007, **27**, p 855–860
14. J. Jarrige, T. Joyeux, J.P. Lecompte, and J.C. Labbe, Influence of Oxygen on the Joining Between Copper and Aluminium Nitride, *J. Eur. Ceram. Soc.*, 2007, **27**, p 337–341

15. O. Dezellus, J. Andrieux, F. Bosselet, M. Sacerdote-Peronnet, T. Baffie, F. Hodaj, N. Eustathopoulos, and J.C. Viala, Transient Liquid Phase Bonding of Titanium to Aluminium Nitride, *Mater. Sci. Eng. A*, 2008, **495**, p 254–258
16. M. El-Sayed, M. Naka, and J.C. Schuster, Interfacial Structure and Reaction Mechanism of AlN/Ti Joints, *J. Mater. Sci.*, 1997, **32**, p 2715–2721
17. M. El-Sayed and M. Naka, Reaction Phases and Strength of AlN/V Diffusion Couples, *J. Mater. Synth. Process.*, 1998, **6**, p 379–386
18. A. Guedes, A.M.P. Pinto, M. Vieira, and F. Viana, Multilayered Interface in Ti/Macor® Machinable Glass-Ceramic Joints, *Mater. Sci. Eng. A*, 2001, **301**, p 118–124
19. A. Elrefaey and W. Tillmann, Correlation Between Microstructure, Mechanical Properties, and Brazing Temperature of Steel to Titanium Joint, *J. Alloy Compd.*, 2009, **487**, p 639–645
20. P. Villars, A. Prince, and H. Kamoto, *Handbook of Ternary Alloy Phase Diagrams*, ASM International, Materials Park, 1994
21. O. Kubaschewski and C. Alcock, *Metallurgical Thermochemistry*, 5th ed., Pergamon Press, Oxford, 1997
22. S. Peteves, Joining Nitride Ceramics, *Ceram. Int.*, 1996, **22**, p 527–533
23. W.F. Ding, Xu. J-H, M. Shen, Fu. Y-C, and B. Xiao, Behavior of Titanium in the Interfacial Region Between Cubic BN and Active Brazing Alloy, *Int. J. Refrac. Met. Hard Mater.*, 2006, **24**, p 432–436
24. W.F. Ding, Xu. J-H, M. Shen, Y.-C. Fu, and B. Xiao, Solid-State Interfacial Reactions and Compound Morphology of cBN Grain and Surface Ti Coating, *Vacuum*, 2006, **81**, p 434–440
25. A. Kar, S. Mandal, K. Venkateswarlu, and A. Ray, Characterization of Interface of Al_2O_3-304 Stainless Steel Braze Joint, *Mater. Character*, 2007, **58**, p 555–562
26. M. Nicholas, Active Metal Brazing, *Br. Ceram. Trans. J.*, 1986, **85**, p 144–146